ECS Journal of Solid State Science and Technology, 2025 **14** 085001

Observation of Atomic-Scale Structural Changes in Al_2O_3/GaN Interfacial Layers Prepared with a Dummy-SiO_2 Process

Jun Uzuhashi,[1,z] Yoshihiro Irokawa,[1,z] Toshihide Nabatame,[1] Tadakatsu Ohkubo,[1] and Yasuo Koide[1,2]

[1]*National Institute for Materials Science, Tsukuba, Ibaraki, 305-0047, Japan*
[2]*Meijo University, Nagoya, Aichi, 468-8502, Japan*

We previously reported that a dummy-SiO_2 process improved the dielectric/GaN interface properties [Y. Irokawa et al., ECS J. Solid State Sci. Technol. **13**, 085003 (2024)]; however, the improvement mechanism has remained unclear. In this study, the atomic-scale structural changes at Al_2O_3/GaN interfaces prepared with the dummy-SiO_2 process are investigated through aberration-corrected scanning transmission electron microscopy with energy-dispersive X-ray spectroscopy. The results reveal that disordered GaN(O) polarity in the interfacial layer in a sample prepared by the standard process was restored to some extent after the dummy-SiO_2 process, which likely led to the improved interface electrical properties.
 [DOI: 10.1149/2162-8777/adf3e3]

Manuscript received July 2, 2025. Published August 5, 2025.

To lower energy losses in electrical systems such as inverters and converters, researchers have investigated various semiconductor materials other than Si and have found that GaN is one of the most attractive materials because of its wide bandgap (3.4 eV) and well-developed device fabrication processes.[1,2] Among such processes, the formation of a dielectric layer on GaN is important because metal-oxide-semiconductor (MOS) structures play a key role in conventional electrical systems. We previously reported that a dummy-SiO_2 process improved the properties of dielectric/GaN interfaces.[3] The process consists of three steps: First, a SiO_2 layer is deposited on GaN, followed by post-deposition annealing (PDA) at 800 °C under N_2. Second, the SiO_2 layer is removed using a buffered HF solution. Third, a new dielectric layer is deposited again to fabricate the MOS device. In this process, the initially deposited SiO_2 functions as a sacrificial layer. The enhanced crystallinity of GaO_x interfacial layers formed on GaN using this process is presumed to be responsible for improved interface electrical properties such as excellent positive-bias stress test results. Thus far, however, the improvement mechanism has remained unclear because the GaO_x interfacial layer, which is less than a few nanometers thick, is so thin that observing its atomic-scale structure is difficult. However, recent advances in analytical electron microscopy may enable us to observe such a minute structure.[4]

In the present study, the atomic-scale structural changes at Al_2O_3/GaN interfaces prepared using the dummy-SiO_2 process are investigated through aberration-corrected scanning transmission electron microscopy (STEM) with energy-dispersive X-ray spectroscopy (EDS) and the results are compared with those for a sample prepared by the standard process. The results reveal three issues: First, the GaO_x layer contains some amount of N; we therefore refer to this layer as GaN(O) hereafter. Second, the polarity of the GaN(O) layers is not uniform; it is disordered, especially in areas proximate to the Al_2O_3/GaN interface (less than ~1.0 nm from the Al_2O_3) prepared with the standard process. Here, we define "disordered polarity" as the state where O and N atoms are disorderly arranged, with Ga atoms occupying the same positions as in the conventional wurtzite GaN structure (Fig 2i). Third, the disordered GaN(O) polarity in the interfacial layer of a sample prepared by the standard process can be restored to some extent after the dummy-SiO_2 process, which likely led to the improved Al_2O_3/GaN interface properties we previously reported.[3]

Experimental

In the present study, we investigated two types of samples: Al_2O_3/GaN structures fabricated with the standard and dummy-SiO_2 processes. The details of the sample preparation have been reported elsewhere.[3] Atomic-scale cross-sectional high-angle annular dark field (HAADF) and annular bright field (ABF)-STEM analysis with EDS was performed at 200 kV using a Spectra Ultra S/TEM (Thermo Fisher Scientific) for these samples. To ensure the quality of comparisons of STEM results for the two types of samples, all of the STEM lamellae were prepared to have the same thickness of 30 nm via a thickness-controllable technique using a focused-ion-beam (FIB)-scanning electron microscopy (SEM) dual-beam Helios5UX equipped with AutoScript (Thermo Fisher Scientific) while minimizing FIB-induced damage.[5,6]

Results and Discussion

Figure 1 shows HAADF-STEM images of the Al_2O_3/GaN structure fabricated with the (a) standard and (b) dummy-SiO_2 processes. EDS compositional line profiles for Ga, Al, and O at the interfaces as a function of depth from the Al_2O_3 layer toward the bulk GaN region of the (c) standard-processed and (d) dummy-SiO_2-processed samples are also shown. These data were obtained to confirm the GaN(O) layer thickness and oxygen concentration in the layer. In Figs. 1a and 1b, the first to fifth Ga layers are indicated; these layer numbers correspond to those in the EDS profile for Ga in Figs. 1c and 1d. Note that each oscillation of the Ga concentration in Figs. 1c and 1d corresponds to each Ga horizontal atomic line observed in Figs. 1a and 1b, respectively. As shown in Figs. 1c and 1d, the Ga concentration saturates near the seventh layer for both processes; therefore, the thickness of the GaN(O) is determined to be 1.5–2.0 nm for both samples. In addition, we found that the oxygen concentration as a function of depth is similar for the two samples. Notably, the detection limit of EDS is on the order of a few percent. Oxygen diffusion from SiO_2 toward GaN during PDA has been previously confirmed;[7] however, we did not observe a difference in the oxygen concentration between the samples, likely because of the oxygen detection limit of EDS.

We next investigated the area proximate to the Al_2O_3/GaN interface. First, we observed a bulk GaN region of the Al_2O_3/GaN structure to confirm that the crystal orientation was in perfect alignment and to enable a comparison of the data for the bulk region with those for the Al_2O_3/GaN interface layers. Figures 2a and 2b show an ABF-STEM image and EDS elemental map, respectively, of the GaN bulk region of the Al_2O_3/GaN structure fabricated with the standard process (depth of approximately 20 nm from the

[z]E-mail: UZUHASHI.Jun@nims.go.jp; IROKAWA.Yoshihiro@nims.go.jp

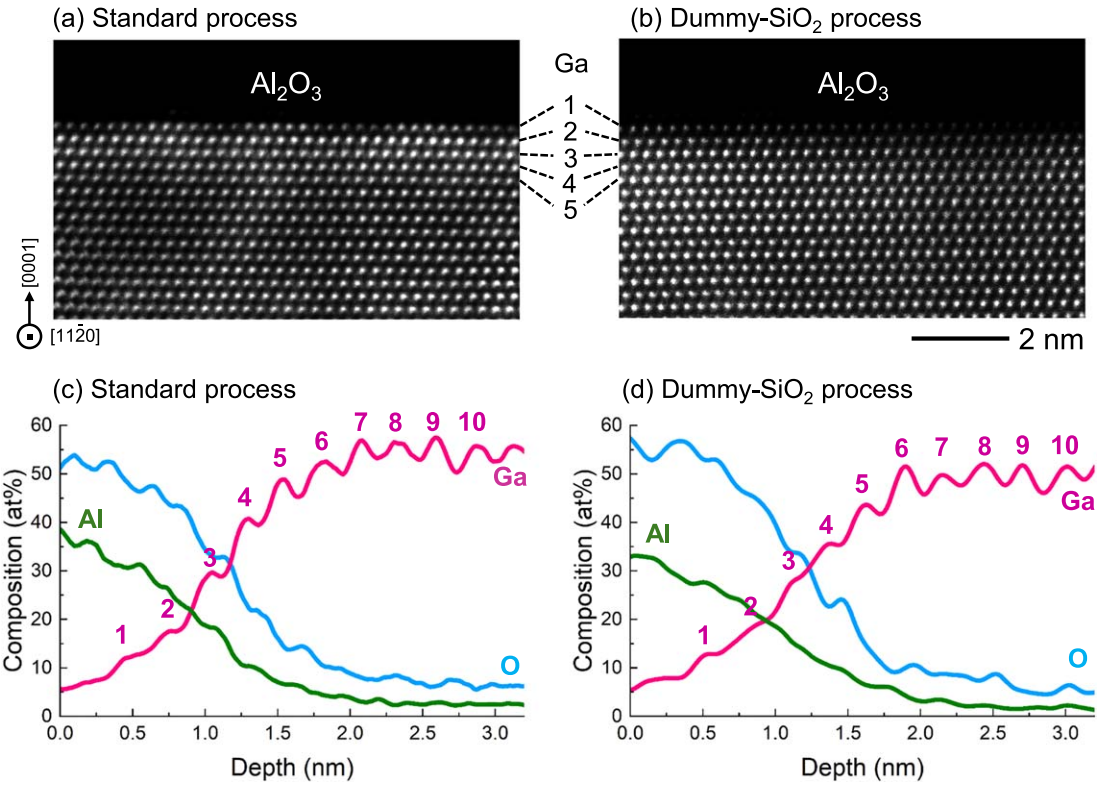

Figure 1. HAADF-STEM images of the Al_2O_3/GaN structure fabricated with the (a) standard and (b) dummy-SiO_2 processes, and the EDS compositional line profiles for Ga, Al, and O at the interfaces as a function of depth from Al_2O_3 layers toward GaN bulk regions of the (c) standard-processed and (d) dummy-SiO_2-processed samples.

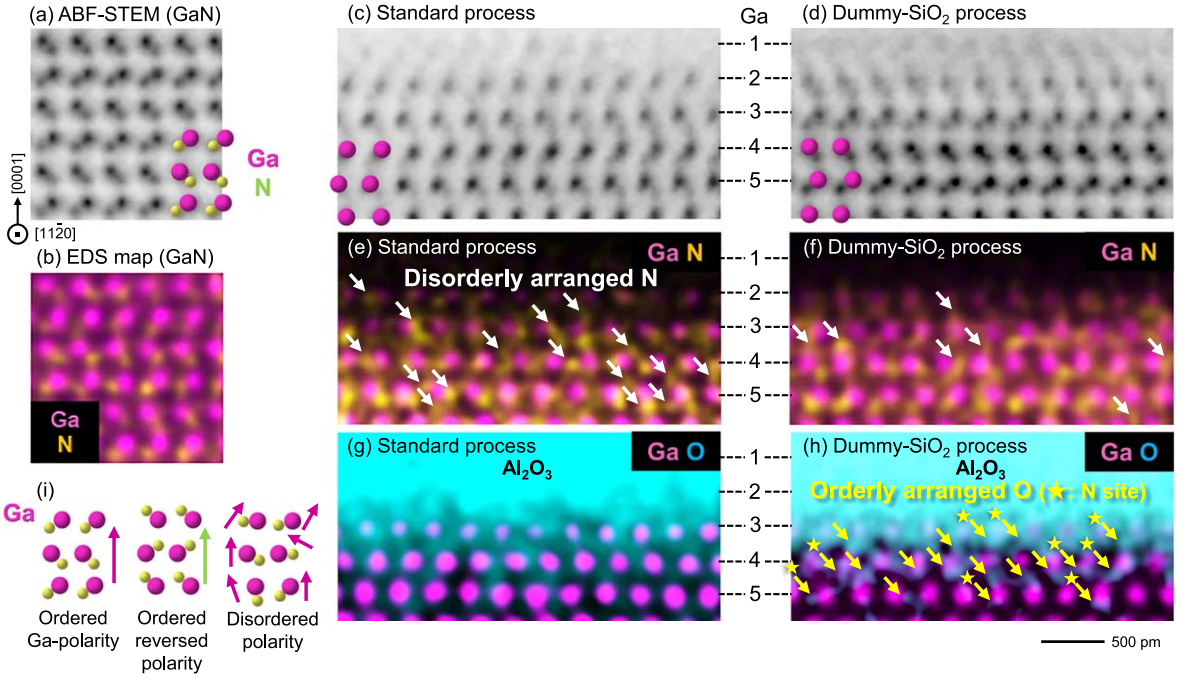

Figure 2. (a) ABF-STEM image and (b) EDS elemental map of the GaN bulk region of a Al_2O_3/GaN structure fabricated with the standard process. ABF-STEM images of Al_2O_3/GaN interfaces for (c) standard-processed and (d) dummy-SiO_2-processed samples. EDS elemental maps of Ga and N for (e) the standard-processed and (f) dummy-SiO_2-processed samples. EDS elemental maps of Ga and O for (g) the standard-processed and (h) dummy-SiO_2-processed samples. (i) Schematic of the polarities.

interface). Larger spherical areas of dark contrast in the ABF-STEM image in Fig. 2a represent Ga atoms, which are colored purple in Fig. 2b. However, ABF-STEM imaging also enabled the visualization of light elements; the positions of the N atoms were observed as smaller spherical regions of dark contrast in the ABF-STEM image (Fig. 2a), and the N atoms are represented as yellow spheres in the EDS elemental map (Fig. 2b). For easier understanding, some of the atomic arrangements of Ga and N atoms are schematically

represented by purple and yellow spheres in Fig. 2a. Figures 2a and 2b show the Ga-polar GaN crystal is oriented toward the surface (the upward direction in the present paper).

ABF-STEM imaging and EDS elemental mapping were applied to the Al_2O_3/GaN interfaces of the standard-processed and dummy-SiO_2-processed samples. The results are shown in Figs. 2c–2h. Specifically, Figs. 2c and 2d show ABF-STEM images of Al_2O_3/GaN interfaces for the standard-processed and dummy-SiO_2-processed samples, respectively. Figures 2e and 2f show EDS elemental maps of Ga and N for the standard-processed and dummy-SiO_2-processed samples, respectively. Figures 2g and 2h show the EDS elemental maps of Ga and O for the standard-processed and dummy-SiO_2-processed samples, respectively. In these figures, the first to fifth Ga layers from Al_2O_3 are indicated, as in Fig. 1. As shown in Figs. 2c and 2d, Ga atoms are observed as larger spheres at the same position as in the bulk GaN region and smaller dark spheres are also apparently observed at the same position as in the bulk GaN region. (Some Ga atoms are schematically represented by purple spheres in Figs. 2c and 2d, as in Fig. 2a). Notably, however, the smaller dark spheres in Figs. 2c and 2d appear cloudy compared with those corresponding to the bulk GaN region (Fig. 2a), suggesting that these atomic arrangements in a few atomic layers near the GaN surface vary from the atomic arrangement in the original Ga-polar crystal structure. In addition, the images of the smaller dark spheres shown in Fig. 2c are much blurrier than those shown in Fig. 2d, indicating that the polarity of the standard-processed sample is less uniform than that of the dummy-SiO_2-processed sample. To investigate the local polarity, we carried out EDS elemental mapping.

First, the EDS elemental maps in Figs. 2e–2h show that the interface layers are composed of GaN(O) instead of pure GaO_x. In the interfacial layers, the O content gradually decreases toward the bulk GaN region, whereas the N content steadily increases with increasing distance from the surface, as described later in the discussion of Fig. 3. The atomic composition ratio between O_x and N_y, i.e., the x/y value, changed from 5.0 to 0.3 toward the GaN bulk in the GaN(O) regions shown in Fig. 2, indicating that O diffusion progresses along the depth direction. Note that this value could be considered a slight overestimation because both sides of the thin STEM lamellae were naturally oxidized during the transfer of the sample for observation. The thicknesses of the GaN(O) layers—that is, N–O intermixing or O diffusion into GaN—are 1.5–2.0 nm for both of the samples (Fig. 1). The presence of N in GaO_x layers has been reported in a study of the early stages of thermal oxidation of GaN.[8]

Second, the EDS elemental maps in Figs. 2e–2h reveal the minute atomic arrangements of Ga, N, and O atoms in the GaN(O) layers. Although no differences are observed in the GaN(O) thicknesses between the two processes, the N and O atomic arrangements are substantially changed via the dummy-SiO_2 process. In Figs. 2e and 2f, Ga atoms are purple and N atoms are orange. The white arrows in Figs. 2e and 2f represent irregular N atom arrangements with respect to the Ga-polar GaN structure. The number of irregular N atom arrangements dramatically decreased when the dummy-SiO_2 process was used. However, for O atoms, the situation is different. In Figs. 2g and 2h, Ga atoms are purple and O atoms are blue. As shown in Fig. 2g, observing a particular O atom site is difficult because the blue region is too vague for the specific atomic positions to be identified, suggesting that most of the O atoms are not located in the ordered specific atomic sites. Conversely, observing O atoms in Fig. 2h is easier because the O atoms represented by yellow arrows appear relatively well ordered at the atomic scale. In particular, the arrows with a star indicate the positions where O atoms have replaced N atoms in the Ga-polar GaN structure. The previously reported native oxide structure of GaN was similar to that of β-Ga_2O_3 with its O atoms uniformly arranged in an inversion of polarity.[9] However, the presently observed structure for the standard-processed sample is not as uniformly polarized as the previously reported one;[9] rather, the polarity is disordered. Figure 2i shows a schematic of the polarities discussed here.

Figures 3a and 3b show normalized EDS signal intensity line profiles for Ga, O, and N at the interfaces as a function of depth from the Al_2O_3 layer toward the GaN bulk region of the standard-

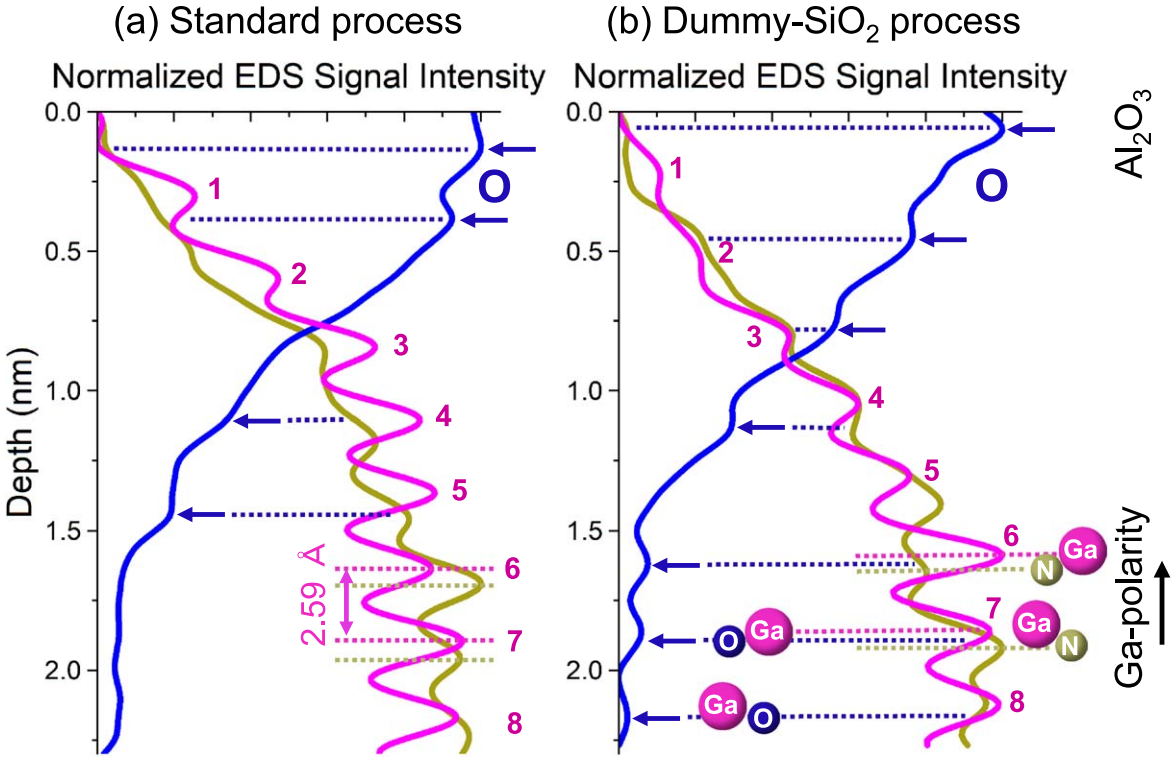

Figure 3. Normalized EDS signal intensity line profiles for Ga, O, and N at the interfaces as a function of depth from Al_2O_3 layers toward the GaN bulk region of (a) the standard-processed and (b) dummy-SiO_2-processed samples.

processed and dummy-SiO_2-processed samples, respectively. The thickness of the GaN(O) layer is found to be 1.5–2.0 nm for both samples, consistent with the data in Fig. 1. In Fig. 3, the numbers on the Ga EDS signal intensity profiles indicate the number of Ga layers counted from the surface; the first to fifth layers correspond to those in Figs. 2c–2h. As shown in Fig. 3, the ratios of O and N gradually vary through the interface layers and are not fixed values. Thus, the GaN(O) layers at the interface do not comprise a single homogenous crystal structure, as previously mentioned. At depths greater than ~1.0 nm, the periodicities and positional relationship of the EDS signal intensity for Ga and N exhibited proximate Ga-polarity for both the standard-processed and dummy-SiO_2-processed samples (Fig. 3). In addition, O atoms are observed at similar positions as N atoms, implying that oxidation progresses with O atoms replacing N atoms while the GaN crystal maintains the same crystal structure and that O atoms might behave as a donor, as we have previously discussed.[10] By contrast, at depths shallower than ~1.0 nm, the signal oscillation for O and N is less clear, meaning that these elements do not occupy ordered positions; this situation is vividly shown in Figs. 2e–2h. However, with careful observation, an indication of a reversed-polarity structure can also be observed in these regions for both samples. A major difference between Figs. 3a and 3b is the distribution of the O atoms. The periodicity of the O intensity, as indicated by the blue arrows, is observed more clearly in Fig. 3b than in Fig. 3a, suggesting that O atoms occupy more ordered positions after the dummy process, consistent with the data shown in Figs. 2g and 2h. Figure 3 also shows that the Ga bond length is apparently greater near Al_2O_3, which may be related to strain at the Al_2O_3/GaN interfaces.

The data obtained in this study demonstrate that the dummy process improves the disordered polarity in the GaN(O) layer to some extent. At this point, however, the relationship between the improvement of the disordered polarity in the GaN(O) layer and the improvement of the interfacial electrical property is unclear. Previously, thin Ga-oxide interlayers were reported to improve the electrical properties in SiO_2/GaN MOS interfaces;[11] the minute structural information about the interface layers would be important for elucidating GaN MOS interface properties. In addition, the reason why the dummy process improves the disordered polarity in the GaN(O) layers is also unclear; even with the dummy process, total restoration of the disordered polarity was not achieved. Therefore, if we develop a more sophisticated polarity control method, it could lead to the realization of interfaces with better electrical properties. Studies of other crystal plane orientations such as m-face might provide hints to a solution.[12]

Conclusions

We investigated the atomic-scale structural changes at Al_2O_3/GaN interfaces prepared with the dummy-SiO_2 process. The results revealed that the disordered GaN(O) polarity in interfacial layers of a sample prepared by the standard process was restored to some extent after the dummy-SiO_2 process. The polarity disorder in the interfacial layer might influence the GaN MOS interfacial electrical properties in a manner similar to the reported effect of grain boundaries on the electrical properties of polycrystalline semiconductors.[13]

Acknowledgments

This research was supported by the Ministry of Education, Culture, Sports, Science and Technology, Japan (MEXT), through its "Creation of Innovative Core Technology for Power Electronics" program under Grant No. JPJ009777 and ARIM (JPMXP1223NM5088). Part of this work was supported by the Electron Microscopy Unit, National Institute for Materials Science (NIMS) and JSPS KAKENHI Grant Numbers 23K03949. The authors thank Kyoko Suzuki for her technical support in preparing STEM lamellae.

ORCID

Jun Uzuhashi https://orcid.org/0000-0003-2023-8158
Yoshihiro Irokawa https://orcid.org/0000-0002-6531-4356

References

1. S. J. Pearton, F. Ren, A. P. Zhang, and K. P. Lee, *Mater. Sci. Eng. R Rep.*, **30**, 55 (2000).
2. T. Kachi, *Jpn. J. Appl. Phys.*, **53**, 100210 (2014).
3. Y. Irokawa, T. Nabatame, T. Sawada, M. Miyamoto, H. Miura, K. Tsukagoshi, and Y. Koide, *ECS J. Solid State Sci. Technol.*, **13**, 085003 (2024).
4. Y. Kozuka et al., *Mater. Today Quantum*, **6**, 100036 (2025).
5. J. Uzuhashi and T. Ohkubo, *Ultramicroscopy*, **262**, 113980 (2024).
6. J. Uzuhashi, Y. Yao, T. Ohkubo, and T. Sekiguchi, *Microscopy (Oxf)*, **74**, dfaf006 (2025).
7. S. J. Pearton, H. Cho, J. R. LaRoche, F. Ren, R. G. Wilson, and J. W. Lee, *Appl. Phys. Lett.*, **75**, 2939 (1999).
8. S. D. Wolter, J. M. DeLucca, S. E. Mohney, R. S. Kern, and C. P. Kuo, *Thin Solid Films*, **371**, 153 (2000).
9. J. H. Dycus, K. J. Mirrielees, E. D. Grimley, R. Kirste, S. Mita, Z. Sitar, R. Collazo, D. L. Irving, and J. M. LeBeau, *ACS Appl. Mater. Interfaces*, **10**, 10607 (2018).
10. Y. Irokawa, K. Mitsuishi, T. Izumi, J. Nishii, T. Nabatame, and Y. Koide, *ECS J. Solid State Sci. Technol.*, **12**, 085003 (2024).
11. T. Yamada, J. Ito, R. Asahara, K. Watanabe, M. Nozaki, T. Hosoi, T. Shimura, and H. Watanabe, *Appl. Phys. Lett.*, **110**, 261603 (2017).
12. M. Hara, T. Nabatame, Y. Irokawa, T. Sawada, M. Miyamoto, H. Miura, T. Kimoto, and Y. Koide, *Mater. Sci. Semicond. Process.*, **196**, 109606 (2025).
13. F. Greuter and G. Blatter, *Semicond. Sci. Technol.*, **5**, 111 (1990).